EFFECTS OF SLIDING FORCE ON MODE I FATIGUE CRACK GROWTH

Xiao-bo YU and Andras ABEL
School of Civil and Mining Engineering , The University of Sydney
NSW 2006, Australia

ABSTRACT

Mode I dominated fatigue crack growth has been studied under non-proportional biaxial stress state. In a notched thin-wall tubular specimen, fatigue crack has been initiated by axial loading, which then propagated along the circumference. At that stage sliding force was introduced by applying static or low frequency torque. As a result the crack growth rate declined and within a transition period the degree of retardation showed a strong dependence on the axial load ratio and the type of torque applied. Macro crack path deviation was observed following the application of static sliding force which amounted to more than 10^{o}. Fatigue crack propagation direction, as predicted by criteria derived from proportional loading conditions, fails to account for this observation. On the other hand, with the application of low frequency torque no macro path crack deviation was observed in the current tests.

KEYWORDS: biaxial fatigue, crack propagation, growth rate retardation, crack path deviation.

INTRODUCTION

Most service fatigue failures involve multiaxial loading, where the fracture mechanics approach is not, as yet, as successful as expected on the basis of work carried out by Paris, Gomez and Anderson (1961) and Paris and Erdogan (1963). The concept of ΔK-dependency in multiaxial fatigue crack growth (FCG) studies is questioned in the literature as shown by Kitagawa *et al* (1985). Although biaxial / multiaxial fatigue crack growth studies are increasing in number, there are only limited number of studies on non-proportional biaxial/multiaxial fatigue crack growth as shown by Pei *et al* (1989) and Brown *et al*(1994).

The main difference between non-proportional and proportional fatigue relates to the co-ordination of loading on the different axes and changing of the direction of principal axes may lead to gross errors when the multiaxial fatigue fracture criteria, as derived from proportional loading condition, is applied (Macha, 1989).

In the present work an attempt is made to contribute towards a better understanding of the differences between proportional and non-proportional loading response. Fatigue crack growth studies in notched thin-wall tubular specimens subjected to non-proportional torque and axial loading have been carried out and the results are discussed below.

SPECIMENS AND MATERIAL

Contrary to proportional FCG studies, two or more separate load sources are needed to achieve non-proportional tests. They can be either tension-compression like in the cruciform test specimen (Brown and Miller, 1985), or tension-compression with the application of torque like in thick center-cracked plate specimen tests (Otsuka, 1980) and notched thin-wall tubular test specimen (Yokobori *et al*, 1985, 1986, 1990).

In the present work, notched thin-walled tubular specimens were used along the lines of Ewing and Williams (1974) who first introduced notched tubular specimen in order to produce data on fracture characteristics. Unlike Yokobori *et al* (1985, 1986, 1990) who adopted small size tubes with 14 mm outer diameter and 1.5 mm thickness, 57.5 mm outer diameter and 1.5 mm thickness tubes were used in the present study. The large diameter-to-thickness ratio of 38 helps to eliminate the effect of uneven through-thickness distribution of shear stresses that may otherwise occur in tubes with small diameter-to-thickness ratio.

Specimen details are shown in Fig. 1 together with the notch dimensions. The tolerance between plugs and tube was filled with Araldite epoxy adhesive. Theoretical analysis and strain gauge measurement showed that no additional stresses were introduced by the limited tolerance. A 60.3 mm x 3.9 mm seamless carbon steel pipe, manufactured according to ASTM standard A106-93 Grade B, was used in the as-received condition. Its metallurgical micro-structure is shown in Fig. 2 and its chemical composition and mechanical properties, as provided by the certificate, is listed in Table 1 and 2 respectively.

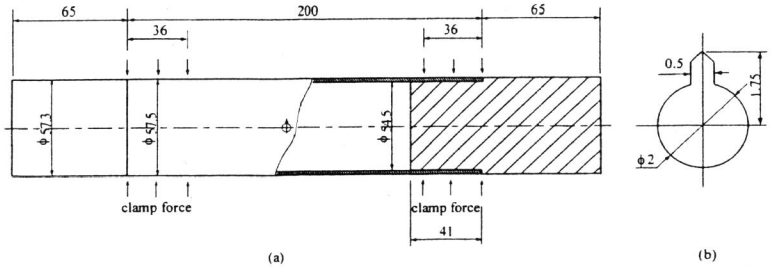

Fig. 1 (a) Illustration of the specimen; (b) detail of crack starter notch.

The single sided crack starter notch was prepared by drilling and electric discharge machining located at the mid-length of the tube. The term "crack length" is defined as the sum of crack starter notch length and fatigue generated crack length as projected on the circumference. It was demonstrated by Broek (1982) that the geometrical detail of the hole can be ignored when the single sided crack length approaches twice the value of the hole diameter. For this reason,

pre-cracks with 6.3 mm in length were fatigue generated before crack growth data recording commenced.

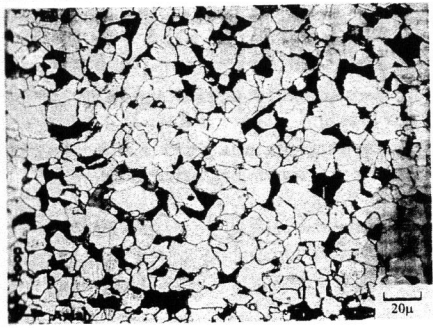

Fig. 2 Metallurgical micro-structures of the material.

Table 1. Chemical Composition

C	Si	Mn	P	S
0.190	0.240	0.56	0.018	0.008
Cu	Cr	Ni	Mo	V
0.050	0.060	0.030	0.010	0.004

Table 2. Mechanical Properties

Proof Strength	Tensile Strength	Elongation in 50mm
399 MPa	500 MPa	34.0%

TEST PROCEDURES

The 8503 type electro-hydraulic Instron Biaxial machine with ±250 KN linear and ±2000 N-m rotary axis capacity was used for the tests. Strain gauges were used to check specimen alignment and no results are reported for cases where the bending stresses were larger than 5%.

Tests were carried out at room temperature under constant load amplitudes and closed loop control, starting with axial loading for fatigue crack initiation and propagation. The operational axial load range definition is in accordance with ASTM Standard E647-88a (1990): $\Delta P = P_{max} - P_{min}$ for $R > 0$ and $\Delta P = P_{max}$ for $R < 0$, where R is defined as the ratio of P_{min} to P_{max}. In all the tests 10 Hz sinusoidal axial cyclic loading was applied with a constant 26.4 KN amplitude, however for the various tests the load ratio varied as 0.2, 0.0 and -0.2. Sliding forces were introduced by torque as: 0.0 to 360.0 N-m at 0.01 Hz when one sided sinusoidal pulsing was applied or at 360.0 N-m when torque was statically applied.

The 26.4 KN axial load and 360 N-m torque are respectively equivalent to 100 MPa tensile stress and 50 MPa as against the transverse cross section of an integral tube.

Pre-cracking - till approximately 6.3 mm crack length - commenced with the application of 100 MPa cyclic loading. The same cyclic tensile amplitude was maintained throughout the mixed mode cycling, and indeed for all of the tests. Crack gauges combined with visual observation were used for the crack growth rate determination which commenced only after the pre-cracking limit was reached.

As only one sided fatigue crack growth was studied, the possibility of crack initiation from the opposite side of the crack starter notch was not ignored and it was found that a second crack developed opposite on the smooth edge of the hole only at around 15 mm crack length. For this reason, the data reported in this paper is limited to 11 mm crack length that is for approximately 5 mm crack extension.

A total of 10 tests were performed as detailed below,

Test No. 1-2 and 3, T1-T2-T3, were run in Mode I fatigue, 10 Hz and 100 MPa operational stress range, till the target crack lenght of 11mm was reached. The variation here related to the R value.

Test No. 4-5 and 6, T4-T5-T6, were run in the same way as T1-T2-T3 to approximately 8.8 mm crack length when 360.0 N-m static torque was superimposed and axial cycling continued. The variation here also related to the R value.

Test No. 7-8 and 9, T7-T8-T9, were run similarly to the previous tests when at approximately 8.8 mm crack length a zero to 360.0 N-m sinusoidal torque was introduced with 0.01 Hz frequency.

Test No. 10, T10, was run from the beginning, that is from fatigue generated crack length equal to zero, at R=0 and cyclic stress of 100 MPa with an applied static torque equal to 360.0 N-m. When the crack length reached approximately 8.8 mm the torque was reduced to zero and cycling continued.

RESULTS

The graphical presentation of the results are shown in Fig. 3 to Fig. 8 and these will be introduced one by one with the appropriate comments.

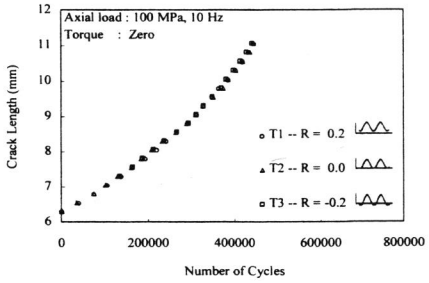

Fig. 3 Mode I crack propagation

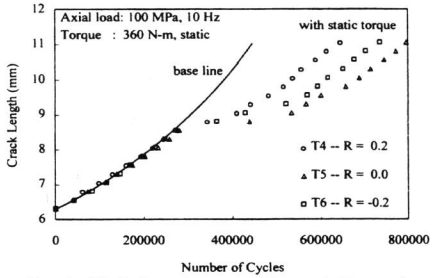

Fig. 4 Mode I crack propagation as influenced by an applied static torque.

Figure 3 demonstrates crack propagation behaviour under Mode I condition. It is clear from these results that the used R variation, from zero to ±0.2, has hardly, if any, effect on the crack propagation rate. This behaviour is reinforced by the following tests, as shown in Figs. 4 and 6, where identical cyclic conditions were applied up to approximately 8.8 mm crack lengths and the three responses were just about equal.

Figure 4 presents the effects of applied static torque. These results show: a) an interim crack propagation period when the static torque is introduced; b) a long term crack propagation retardation associated with the torque and c) an R dependence in the changes brought about by the application of the torque. Note that at R=0 the fatigue performance is better than at R= -0.2, while not surprisingly the least amount of torque benefit is derived at R=0.2. With the introduction of torque fatigue crack path deviation took place, from the circumference, to a direction where tensile normal stress was resulted as resolution of the applied torque. The

deviated crack paths came out to be parabola-like curves with a large radius as shown in Fig. 5(a). The largest tangential angles along the curved crack paths were found at the beginning of crack deviation, which amounted to more than 10°. The reported data were obtained by the use of a 50 times magnification.

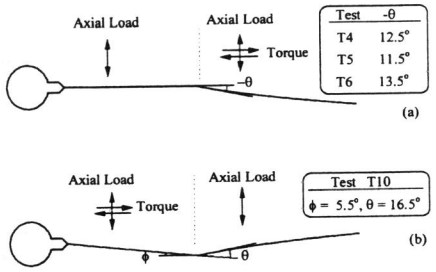

Fig. 5 Illustration of fatigue crack path deviation: (a) in Test T4, T5 and T6; (b) in Test T10.

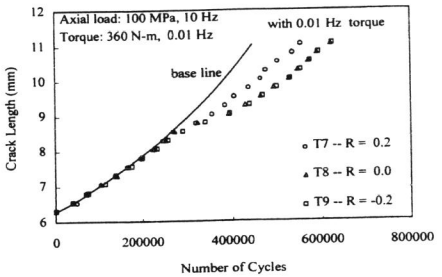

Fig. 6 Mode I crack propagation as influenced by applied low frequency torque.

Figure 6 shows, with the introduction of the 0.01Hz frequency torque, that: a) the transition period is shorter when compared with those observed at constant torque; b) crack growth retardation is not as great as with constant torque; c) at R=0 and R=-0.2 the application of low frequency torque leads to, approximately, the same crack retardation benefit and d) the crack retardation is smallest at R=0.2. In these three tests no crack path deviation was observed when the cyclic torque was introduced.

To compare the relative benefit obtained by the applied static and low frequency torque, Fig. 7 becomes useful. Excepting the transition period, the long term FCG retardation shows similar tendencies when the different R values and different applied torque are compared.

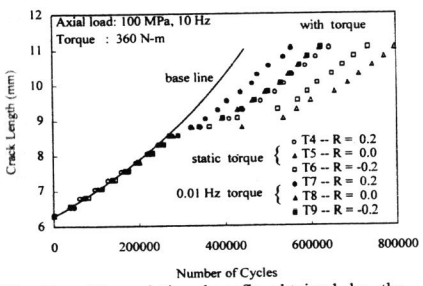

Fig. 7 The relative benefit obtained by the application of torque.

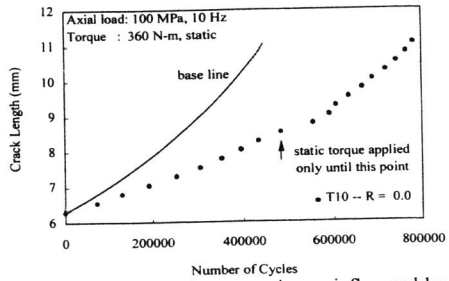

Fig. 8 Mode I crack propagation as influenced by applied static torque from the very beginning.

In test 10 the sliding force was applied from the beginning and from the result, as shown in Fig. 8 it is clear that: a) crack propagation retardation takes place while static torque is applied and b) partial recovery of crack growth rate commences when the torque is reduced to zero.

The crack path deviation in this test is illustrated in Fig. 5(b). The first part, with static torque applied, appeared nearly straight and deviated in the direction compatible with the tensile

normal stresses resolved from the applied torque. The second part, no torque applied, deviated into the opposite direction with a tendency of blending into a circumference crack path.

DISCUSSIONS

Two major aspects are discussed below relating to crack growth retardation and crack path deviation.

Crack Growth Retardation

Crack growth retardation behaviour within the transition period is relevant to crack closure. With the application of torque, significant Mode II deformation operates at the crack tips and therefore premature crack surface contact emerges between the asperities. As the tensile component is responsible for relieving some of the closure caused by sliding forces (Tong *et al*, 1995), it is not surprising to observe the strong retardation dependence on the R values. Accordingly, least retardation was observed in tests where R equals to 0.2. This reasoning does not apply with test T6 (R=-0.2) which exhibited less retardation than test T5 (R=0). The exception can be rationalized by crack path deviation. Once crack path deviation commenced the contributing tensile stresses, as resolved from the torque, lead to a faster crack growth. This explanation is strengthened by the results obtained with the introduction of low frequency torque as similar retardation behaviour took place with T8 (R=0) and T9 (R=-0.2), when no macro crack path deviation occurred.

Crack closure as mentioned above is very similar to the so-called roughness-induced crack closure, which was primarily introduced to explain crack growth behaviour in the near-threshold regime (Suresh and Ritchie, 1982). In the case of near-threshold crack propagation crack closure develops even under remote Mode I condition because of the irreversible Mode II shear deformation along single slip planes (Minakawa and McEvily, 1981). In the current tests, however, which were carried out in Paris regime, crack closure is expected only when mode II deformation is introduced by sliding force.

Since crack closure promoted by Mode II deformation is associated with interference between crack surface asperities, change in the degree of crack growth retardation is expected. This is in line with the observed crack growth retardation which shows a gradual reduction with crack length extension within the transition period. This type of fatigue growth characteristics under mix-mode condition has been also described by Suresh (1992).

Crack growth retardation beyond the transition period appeared to be insensitive to the variation of R values. This phenomenon suggests that there must be other mechanism besides the crack closure accounting for long term retardation. More studies are needed to clarify this mechanism.

Fatigue test results under static torque and cycling axial loading were also reported by Yokobori *et al* (1990), indicating that the static torque had no effect on the crack propagation rate. This maybe explained by the differences in the used torque values. In the present tests nominally 50 MPa shear stress was combined with the axial stress range of 100 MPa, while in Yokobori's test 7.806 MPa shear stress was superimposed on the axial cyclic stress range of

121.6 MPa. This therefore is in full agreement with the reasoning expressed above. A certain level of sliding component is needed to affect the crack closure.

Crack Path Deviation

Several criteria have been proposed to account for crack path deviation under biaxial/multiaxial stress state, such as maximum tangential stress criterion (Erdogan and Sih, 1963), minimun strain energy density criterion (Sih, 1974) and maximum energy release criterion (Hussain *et al*, 1973). These models were proposed primarily for fracture crack path prediction. When they were extended to fatigue crack propagation cases, range of stress values or energy values are substituted in the criteria. Under proportional biaxial stress state, it was found that normally these approaches lead to similar results.

Maximum tangential stress range ($\Delta\sigma_\theta$) criterion suggests crack propagation along the direction as predicted by the following equation,

$$\frac{\partial \Delta\sigma_\theta}{\partial\theta} = 0, \qquad \frac{\partial^2 \Delta\sigma_\theta}{\partial\theta^2} < 0 \tag{1}$$

where θ is direction angle from pre-crack and the tangential stress range, $\Delta\sigma_\theta$, is given as,

$$\Delta\sigma_\theta = \frac{1}{2\sqrt{2\pi r}}\cos\frac{\theta}{2}[\Delta K_I(1+\cos\theta) - 3\Delta K_{II}\sin\theta] \tag{2}$$

In tests T4 and T5, because ΔK_{II} equals zero, no path deviation is predicted by this criteria.

Minimum strain energy density range (ΔS) criterion predicts crack propagation direction by the following formulae,

$$\frac{\partial \Delta S}{\partial\theta} = 0, \qquad \frac{\partial^2 \Delta S}{\partial\theta^2} > 0 \tag{3}$$

where the strain energy density range ΔS is the difference between maximum and minimum strain energy. For the present tests ΔS can be expressed as,

$$\Delta S = 2\Delta K_I[a_{11}K_{I\,mean} + a_{12}K_{II\,static}] \tag{4a}$$

for T4 and T5 whereas for T10,

$$\Delta S = 2\Delta K_I K_{I\,mean}[a_{11} + 2a_{12}t + a_{22}t^2] \tag{4b}$$

where t equals to K_{II}/K_I and coefficients a_{11}, a_{12} and a_{22} are functions of the shear modulus, Poisson ratio and direction angle. Their detailed expression has been published by Sih (1974).

According to eq. (4a), minimum ΔS criterion suggests crack path deviation following the superposition of static torque to axial cycling.

Table 3. Comparison of Crack Path Deviation ($\eta = K_{Icl} / k_{Imax}$)

Test	Current Test Results	maximum $\Delta\sigma_\theta$ ($\eta = 0.0$)	minimum ΔS ($\eta = 0$)	maximum $\Delta\sigma_\theta$ ($\eta = 0.15$)	minimum ΔS ($\eta = 0.8$)
T4	-12.5°	0.0°	-22.1°	—	-18.3°
T5	-11.5°	0.0°	-25.0°	-11.5°	-20.5°
T10	16.5°	11.4°	11.2°	—	—

A comparison of crack path deviation between the experimental results and those predicted by maximum $\Delta\sigma_\theta$ criterion and minimum ΔS criterion is given in Table 3. It is shown for test T4

and T5 that predictions by maximum $\Delta\sigma_\theta$ criterion and minimum ΔS criterion are: firstly different from each other and secondly neither of them is close to the experimental results. In test T10, two criteria led to similar predictions, but these still exhibited some, although smaller, differences when compared with the test results.

It was postulated by Suresh (1992) that "because of crack face contact in mixed Modes I and II, the nominal use of any of the foregoing failure criteria is not likely to provide perfect agreement with experimental observations." However, with the consideration of crack closure in the current tests the disagreement between predictions and test results is still not eliminated. With minimum ΔS criterion, higher K_{Icl} value leads to better prediction. But as shown in Table 3, the predictions are still quite different from the test results even if the crack closure K_{Icl} is taken as high as 80% of K_{Imax}. As with the maximum $\Delta\sigma_\theta$ criterion, a good prediction is achieved in T5 if K_{Icl} is taken as 15% of K_{Imax}. However, the best prediction achieved in T4 is -18.9°, which shows certain difference from the test result of -12.5°. It is thus clear that the nominal use of a criteria is at least not the only cause responsible for its poor prediction. Instead, the disagreement between predicted and experimental crack path deviation suggests that fatigue criteria derived from proportional loading condition are not applicable to non-proportional situation.

Hourlier *et al* (1985) has also realized that the proportional fatigue criteria is not applicable and thus a maximum crack propagation speed model was proposed to predict crack banching direction. However, Hourlier *et al*'s model was based on the assumption that sliding force has no effect on crack propagation speed, which is in contrast with the current observations.

CONCLUSIONS

In the current studies, notched thin-walled tube specimens were used to study the effect of sliding forces on Mode I dominated fatigue crack growth. It was found that,

1) The introduction of static or low frequency sliding forces, in the form of torque, results in the retardation of Mode I dominated fatigue crack propagation.
2) The retardation consists of two phases the first of which is a transient period large in magnitude but it is soon to be overtaken with a steady state crack propagation.
3) The degree of retardation in the transition period is strongly dependent on the R value and on the sliding force style.
4) The retardation behaviour within transition period is relevant to crack closure.
5) More than 10° macro crack path deviation is observed when a static sliding force is superimposed on the Mode I condition. However, no macro path deviation is observed with the application of low frequency torque.
6) Fatigue criteria derived from proportional loading conditions are not applicable to non-proportional loading conditions.

REFERENCES

ASTM standard E647-88a (1990). Standard test Method for measurement of fatigue crack growth rate. *Annual book of ASTM Standards*, Vol. 03.01., pp. 648-668.

Broek, D. (1982). *Elementary Engineering Fracture Mechanics*, Martinus Nijhoff Publishers, The Hague/Boston/London, 3rd Ed., pp. 369-371.

Brown, M. W. and K. J. Miller (1985). Mode I fatigue crack growth under biaxial stress at room and elevated temperature. *Multiaxial Fatigue, ASTM* **853**, K. J. Miller and M. W. Brown, Eds., ASTM, Philadelphia, pp. 135-152.

Brown, M. W., K. J. Miller, U. S. Fernando, J. R. Yates and D. K. Suker (1994). Aspects of multiaxial fatigue propagation. *Fourth International Conference on Biaxial/Multiaxial Fatigue*, St Germain en Laye (France), Vol. 1, pp. 3-16.

Ewing P. D. and J. G. Williams (1974). The fracture of spherical shells under pressure and circular tubes with angled cracks in torsion. *International Journal of Fracture*, Vol. 10, No. 4, pp. 537-544.

Erdogan F. and G. C. Sih (1963). On the crack extension in plates under plan loading and transverse shear. *J. bas Engng Trans.* ASME **85**, 519-527.

Hourlie F., H. d'Hondt, M. Truchon and A. Pineau (1985). Fatigue crack path behavior ubder polymodal fatigue. *Multiaxial Fatigue, ASTM* **853**, K. J. Miller and M. W. Brown, Eds., ASTM, Philadelphia, pp. 228-248.

Hussain M. A. , S. L. Pu and J. Underwood (1973), *ASTM STP* **560**, 2-28.

Kitagawa, H., R. Yuuki, K. Tohgo and M. Tanabe (1985). ΔK-dependency of fatigue growth of single and mixed mode cracks under biaxial stresses. *Multiaxial Fatigue, ASTM* **853**, K. J. Miller and M. W. Brown, Eds., ASTM, Philadelphia, pp. 164-183.

Macha E. (1989). Generalization of fatigue fracture criteria for multiaxial sinusoidal loadings in the range of random loadings. *Biaxial and Multiaxial Fatigue, EGF3*, M. W. Brown and K. J. Miller Eds., Mechanical Engineering Publications, London, pp. 425-436.

Minakawa, K. and A.J. McEvily (1981). On crack closure in the near-threshold region. *Scripta Metallurgia*, **15**, pp. 633-636.

Otsuka A., K. Mori., S. Tsuyama and Y. Sumiya (1980). Fatigue crack growth and threshold under mode II loading. *Proc. Int. Conf. Analytical and Experimental Fracture Mechanics*, Rome, pp. 375-386.

Paris, P. C., M. P. Gomez and W. E. Anderson (1961). A rational analytic theory of fatigue. *The trend in Engineering*, **13**, 9-14.

Paris, P. C. nad F. Erdogan (1963). Critical analysis of crack propagation laws. Trans. ASME, *J. Basic Eng.*, **85**, 528-534.

Pei H. X, M. W. Brown and K. J. Miller (1989). Fatigue crack propagation under complex biaxial stress cycling. *Biaxial and Multiaxial Fatigue, EGF3*, M. W. Brown and K. J. Miller Eds., Mechanical Engineering Publications, London, pp. 587-603.

Sih, G. C. (1974). Strain energy density factor applied to mixed mode crack problems. *Int. J. Fracture* **10**, 305-321.

Suresh, S (1992). *Fatigue of Materials*, Chapter 11, Cambridge University Press, pp. 352-253.

Suresh, S. and R.O. Ritchie (1982). A geometric model for fatigue crack closure induced by fracture surface roughness. *Metall. Trans. A*, **13A**, 1627-1631.

Tong, J., J. R. Yates and M. W. Brown (1995). A model for sliding mode crack closure, part II: mixed mode I and II loading and application. *Engineering Fracture Mechanics*, Vol. 52, No. 4, pp. 613-623.

Yokobori, T. A. Jr., T. Yokobori, K. Sato and K. Shyoji (1985). Fatigue crack growth under mixed modes I and II. *Fatigue Fract. Engng. Mater. Struct.*, **8**, 4, 315-325.

Yokobori, T. A., T. Yokobori, K. Ishii, K. Sato and K. Shyoji (1986). Fatigue crack growth rate and crack initiation and fracture life under mixed modes I and II. *Zairyo/Journal of the Society of Materials Science, Japan*, v. **35**, n.395, pp. 930-935. (in Japanese)

Yokobori, T. A., T. Isogai, T. Yokobori and Y. Koizumi (1990). Effect of stress components on fatigue crack growth rate under multiaxial stress condition. *Zairyo/Journal of the Society of Materials Science, Japan*, v. **39**, n.443, pp. 1106-1112. (in Japanese)